

## Beaming Effect and Relativistic Jet Characteristic in Fermi-era-Blazars

Zhiyuan Pei,<sup>a,b,c,\*</sup> Junhui Fan,<sup>a,b,c</sup> Jianghe Yang,<sup>d</sup> Xiangtao Zeng,<sup>e</sup> Zhuang Zhang,<sup>e</sup> Hubing Xiao,<sup>f</sup> Peizhen Hu,<sup>b</sup> Shuochun Wang<sup>b</sup> and Yanjun Qian<sup>b</sup>

<sup>a</sup>Center for Astrophysics, Guangzhou University, Guangzhou 510006, People's Republic of China

<sup>b</sup>School of Physics and Materials Science, Guangzhou University, Guangzhou 510006, People's Republic of China

<sup>c</sup>Astronomy Science and Technology Research Laboratory of Department of Education of Guangdong Province, Guangzhou 510006, People's Republic of China

<sup>d</sup>Department of Physics and Electronics Science, Hunan University of Arts and Science, Changde 415000, People's Republic of China

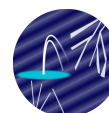
<sup>e</sup>School of Physics and Astronomy, Sun Yat-Sen University, Zhuhai 519082, People's Republic of China

<sup>f</sup>Shanghai Key Lab for Astrophysics, Shanghai Normal University, Shanghai 200234, People's Republic of China

E-mail: [peizy@gzhu.edu.cn](mailto:peizy@gzhu.edu.cn), [fjh@gzhu.edu.cn](mailto:fjh@gzhu.edu.cn)

Employing the beaming effect we present an effective method by means of the beaming effect to estimate four crucial parameters, including the central black hole mass  $M_{\text{BH}}$ , the Doppler factor  $\delta$ , the location of  $\gamma$ -ray-emitting region  $R_\gamma$ , and the propagation angle with respect to the axis of the accretion disk  $\phi$ , for a large sample of  $\gamma$ -ray blazars. We put forward an updated demarcation between BL Lacs and FSRQs based on the relation between broad-line region luminosity and disk luminosity both measured in Eddington units, i.e.,  $L_{\text{disk}}/L_{\text{Edd}} = 4.68 \times 10^{-3}$ , indicating that there are some differences between BL Lacs and FSRQs on the accretion power in the disk. By adopting a two-component model of emission within jets, we successfully separated the emission of radio, X-ray, GeV and TeV into beamed and unbeamed contributions for the largest sample of Fermi blazars up to now. Our results suggest that the emission is mainly from the core/beamed component in  $\gamma$ -ray blazars. Based on the study of jet power and launching in blazars, our results suggest that BL Lac jets are powered by extracting black hole rotation energy, while FSRQ jets are mostly powered by accretion disks. Most of FSRQs can be explained by the Blandford-Payne mechanism, while most of BL Lacs can be explained by the Blandford-Znajek mechanism.

39th International Cosmic Ray Conference (ICRC2025)  
15–24 July 2025  
Geneva, Switzerland



**ICRC 2025**  
The Astroparticle Physics Conference  
Geneva July 15-24, 2025

\*Speaker

## 1. Introduction

Blazars exhibiting distinctive and extreme observational properties, such as large amplitude and rapid variability, superluminal motion, high polarization, and strong emission over the entire electromagnetic spectrum. All of these properties are due to the relativistic beaming effect [1, 2]. According to the optical emission line features, blazars can be divided into flat spectrum radio quasars (FSRQs) and BL Lacertae objects (BL Lacs), where BL Lacs have weak or no emission lines (i.e. the equivalent width, EW, of the emission line in rest frame is less than  $5 \text{ \AA}$ ), while FSRQs show stronger emission lines  $EW \geq 5 \text{ \AA}$  in their optical spectra. From the transition between FSRQs and BL Lacs, and based on the luminosity of the broad-line region (BLR) measured in Eddington units, Ghisellini et al. (2011) [3] proposed a physical distinction between these classes, setting the dividing line of  $L_{\text{BLR}}/L_{\text{Edd}} \sim 5 \times 10^{-4}$ .

Based on a relativistic beaming model, the total emission from AGNs consists of two components, namely, a beamed component and an unbeamed one. Then, the observed total luminosity,  $L^{\text{tot}}$ , is the sum of the beamed,  $L_{\text{b}}$ , and unbeamed,  $L_{\text{unb}}$  contributions, i.e.  $L^{\text{tot}} = L_{\text{b}} + L_{\text{unb}}$ . In the radio band, the ratio of the two components,  $R_{\text{radio}}$ , is defined as the radio core-dominance parameter, i.e.  $R_{\text{radio}} = L_{\text{b}}/L_{\text{unb}}$  [4]. This ratio can also be expressed as:

$$R(\phi) = \frac{\text{flux density of beamed compact core}}{\text{flux density of unbeamed components}}, \quad R_{\perp} = R(90^\circ), \quad (1)$$

where  $\phi$  is the viewing angle between the line-of-sight and the motion direction of the approaching side of the compact core and  $R_{\perp}$  refers to the ratio of the luminosity in the jet to the unbeamed luminosity when  $\phi = 90^\circ$ . The compact core is assumed to be produced by emission from the unresolved bases of two oppositely directed jets moving with speed  $\beta c$  relative to the central object, where  $\beta$  is the relativistic bulk velocity in units of the speed of light  $c$ .

Previous studies have shown that the radio core-dominance parameter  $R_{\text{radio}}$  can play the role of a tracer of the beaming effect,  $R_{\text{radio}} = f\delta^p$ , where  $f$  is the intrinsic ratio, defined by the intrinsic flux density of the jet to the extended flux density in the co-moving frame,  $f = \frac{S_{\text{core}}^{\text{in}}}{S_{\text{ext.}}^{\text{in}}}$ .  $\delta$  is the Doppler factor,  $p = n + \alpha$ ,  $\alpha$  is the radio spectral index and  $n$  depends on the shape of the emitted spectrum and the physical details of the jet, being  $n = 2$  for a continuous jet and  $n = 3$  for a moving blob. The Doppler factor  $\delta$  is  $\delta = [\Gamma(1 - \beta \cos \phi)]^{-1}$ , where  $\Gamma$  is the Lorentz factor defined as  $\Gamma = (1 - \beta^2)^{-1/2}$ . Then, the radio core-dominance parameter can be written as  $R_{\text{radio}} = f\delta^p = f[\Gamma(1 - \beta \cos \phi)]^{-p}$ . When the viewing angle  $\phi$  is large ( $\phi \gtrsim \arccos[0.5/\beta]$ ), the emission from the receding jet is no longer negligible, and the relation becomes

$$R_{\text{radio}} = f\Gamma^{-p} [(1 - \beta \cos \phi)^{-p} + (1 + \beta \cos \phi)^{-p}]. \quad (2)$$

The *Fermi* Gamma-ray Space Telescope with its main instrument on-board, the Large Area Telescope (*Fermi*-LAT), opened a new era in the study of high-energy emission from AGNs. Many new high-energy  $\gamma$ -ray sources were detected, revolutionising, in particular, the knowledge of  $\gamma$ -ray blazars, providing us with a valuable opportunity to explore the  $\gamma$ -ray production mechanism. Based on the first ten years of data from the *Fermi* Gamma-ray Space Telescope mission, the latest catalog, 4FGL, or the fourth *Fermi* Large Area Telescope catalog of high-energy  $\gamma$ -ray sources, has been released, which includes 5778 sources above the significance of  $4\sigma$ , covering the 50 MeV–1 TeV

range [5]. AGNs are the vast majority of sources in 4FGL; among them 3421 blazars, or 1191 BL Lacs, 733 FSRQs, and 1498 blazar candidates of unknown class (BCUs).

Since the radiation of blazars is dominated by the emission from the relativistic jet, the jet formation mechanism in blazars has long been a prosperous problem in astrophysics and has been studied by many authors. Blandford & Znajek (1977)[6] proposed that the relativistic jet extracts the rotation energy of black hole, as known as Blandford-Znajek (BZ) mechanism. In this scenario, the jet power depends on the spin and mass of the black hole. Also, Blandford & Payne(1982) [7] suggested that the jet power is extracted from the rotation energy of accretion disk, as known as Blandford-Payne (BP) mechanism. Recently, Xiao et al. (2022) [8] suggested that the jet formation in FSRQ might be dominated by the BP mechanism while BL Lacs are likely powered through the BZ mechanism.

## 2. Method

### 2.1 Physical Parameters Estimation

It is generally believed that the escape of high energy  $\gamma$ -rays from AGNs depends on the  $\gamma$ - $\gamma$  pair production process since plenty of soft photons are surrounding the central black hole. Therefore, we can use the opacity of  $\gamma$ - $\gamma$  pair production to constrain the fundamental physics parameters for  $\gamma$ -ray blazars. The  $\gamma$ -rays are constrained in a solid angle, i.e.,  $\Omega = 2\pi(1 - \cos \Phi)$ , yielding that the apparent observed  $\gamma$ -ray luminosity can be expressed as  $L_{\gamma}^{\text{obs}} = \Omega d_L^2 F_{\gamma}^{\text{obs}}$ , where  $d_L$  denotes the luminosity distance and  $F_{\gamma}^{\text{obs}}$  is the observed  $\gamma$ -ray flux. The observed  $\gamma$ -rays from AGNs require that the jet almost points to us and the optical depth  $\tau$  is not greater than unity, i.e.,  $\tau \leq 1$ . Since the  $\gamma$ -rays come from a solid angle  $\Omega$  instead of being isotropic then the non-isotropic radiation, thus the absorption and beaming effects should be considered when the properties of a  $\gamma$ -ray-loud blazars are discussed. Besides, the variability time scale also affects the  $\gamma$ -ray emission region. All of all, based on these considerations, we deduce an effective method to derive four fundamental physics parameters including the upper limit of the central black hole mass ( $M$ ), the Doppler factor ( $\delta$ ), the distance along the axis to the site of the  $\gamma$ -ray production ( $d$ ) and the propagation angle ( $\Phi$ ) for selected *Fermi*-LAT detected blazars. Four equations are obtained[9].

$$\begin{aligned} \frac{d}{R_g} &= 1730 \times \frac{\Delta T_D}{1+z} \delta M_7^{-1}, \\ L_{\text{iso}}^{45} &= \frac{2.52 \lambda \delta^{\alpha_{\gamma}+4}}{(1 - \cos \Phi)(1+z)^{\alpha_{\gamma}-1}} M_7, \\ 9 \times \Phi^{2.5} \left( \frac{d}{R_g} \right)^{-\frac{2\alpha_X+3}{2}} + k M_7^{-1} \left( \frac{d}{R_g} \right)^{-2\alpha_X-3} &= 1, \\ 22.5 \times \Phi^{1.5} (1 - \cos \Phi) - 9 \times \frac{2\alpha_X+3}{2\alpha_{\gamma}+8} \Phi^{2.5} \sin \Phi - \frac{2\alpha_X+3}{2\alpha_{\gamma}+4} k M_7^{-1} A^{-\frac{2\alpha_X+3}{2}} (1 - \cos \Phi)^{-\frac{2\alpha_X+3}{2\alpha_{\gamma}+8}} \sin \Phi &= (9) \end{aligned}$$

### 2.2 $\gamma$ -ray core-dominance parameter

The parameters  $R_{\perp}$ ,  $f$ , and  $\Gamma$  is given by:

$$R_{\perp} = \frac{2f}{\Gamma^p}. \quad (4)$$

After substituting for parameter  $f$  and considering flat-spectrum radio AGNs (i.e.  $\alpha = 0$ , resulting in  $p = 2$ ), the relation (2) can be expressed as:

$$R_{\text{radio}} = R_{\perp} \frac{1}{2} \left[ (1 - \beta \cos \phi)^{-2} + (1 + \beta \cos \phi)^{-2} \right], \quad (5)$$

where the second term on the right-hand side originates from a “counter-jet”. If one defines  $g(\beta, \phi) = \frac{1}{2} \left[ (1 - \beta \cos \phi)^{-2+\alpha} + (1 + \beta \cos \phi)^{-2+\alpha} \right]$ , then equation (5) can be reduced to  $R = R_{\perp} g(\beta, \phi)$  ( $\alpha = 0$ ). For a source, if the values of  $\beta$ ,  $\phi$  and  $R_{\text{radio}}$  are given, one can obtain  $R_{\perp}$  from equation (5). In this work, we take the value  $R_{\perp} = 0.024$  as concluded by Orr & Browne (1982) [10].

We adopt the two-component model in the X-ray,  $\gamma$ -ray and TeV emission, respectively [11–13]. We only present the example of  $\gamma$ -ray emission. In this scenario, the ratio of the beamed radio emission in the transverse direction to the extended radio emission is considered to be constant. Thus it is expected that the transverse beamed  $\gamma$ -ray luminosity,  $L_{\gamma, \text{b}\perp}$  is proportional to the extended radio emission,  $L_{\text{r, unb}}$ , i.e.  $L_{\gamma, \text{b}\perp} = A \cdot L_{\text{r, unb}}$ , where  $A$  is a constant. Similar to the radio beaming factor, we can define a parameter, namely the  $\gamma$ -ray beaming factor  $g_{\gamma}(\beta, \phi)$ , as

$$g_{\gamma}(\beta, \phi) = \frac{1}{2} \left[ (1 - \beta \cos \phi)^{-(2+\alpha_{\gamma})} + (1 + \beta \cos \phi)^{-(2+\alpha_{\gamma})} \right], \quad (6)$$

where  $\alpha_{\gamma}$  is the  $\gamma$ -ray spectral index of the beamed emission ( $\alpha_{\gamma} = \alpha_{\gamma}^{\text{ph}} - 1$ ). Therefore, the beamed luminosity for an inclination angle  $\phi$  between the jet direction and the line of sight is  $L_{\gamma, \text{b}}(\phi) = g_{\gamma}(\beta, \phi) L_{\gamma, \text{b}}(90^{\circ})$ . We now define the ratio of the beamed to unbeamed  $\gamma$ -ray luminosity, the  $\gamma$ -ray core-dominance parameter, as:

$$R_{\gamma} = \frac{L_{\gamma, \text{b}}}{L_{\gamma, \text{unb}}} = R_{\gamma\perp} g_{\gamma}(\beta, \phi), \quad R_{\gamma\perp} = \frac{L_{\gamma, \text{b}}(90^{\circ})}{L_{\gamma, \text{unb}}}, \quad (7)$$

where  $R_{\gamma\perp}$  is the ratio of the beamed to the unbeamed  $\gamma$ -ray component.

Using the determination by minimizing  $\Sigma[\log(L_{\gamma}/L_{\gamma}^{\text{obs}})]^2$  for all the sources, we can obtain  $R_{\gamma\perp} = 3.05 \times 10^{-3}$ . Similarly, we can also ascertain  $R_{\text{X}\perp} = 2.27 \times 10^{-3}$  and  $R_{\text{TeV}\perp} = 1.60 \times 10^{-4}$  for the X-ray and TeV emission respectively. Then, given the radio core-dominance parameter,  $R_{\text{radio}}$ , we can obtain  $\beta \cos \phi$  from equation (5) using  $R_{\perp} = 0.024$  [10]. This in turn gives the  $\gamma$ -ray beaming factor  $g_{\gamma}(\beta, \phi)$  via equation (6) and the core-dominance parameter in X-ray,  $\gamma$ -ray and TeV bands [11–13], and finally calculate the core-dominance parameter in these bands using equation (7).

### 2.3 Jet Model and Launching

In the framework of the Blandford-Znajek (BZ) model, driven by a rapidly spinning black hole, the jet power can be calculated as described by [8, 14]:

$$P_{\text{jet}}^{\text{BZ}} = \frac{1}{32} \omega_{\text{F}}^2 B_{\text{h}}^2 R_{\text{h}}^2 c j^2. \quad (8)$$

The variables in this equation represent the following:  $\omega_{\text{F}}$  denotes the field lines angular velocity relative to the black hole angular velocity,  $B_{\text{h}}$  signifies the field strength at the black hole horizon

$R_h$ , and  $j$  stands for the black hole spin. The maximum jet power within the BZ model framework can be derived:

$$P_{\text{jet}}^{\text{BZ}} = 39 \times 10^{36} \omega_F^2 \beta \tau_c m r_h^{-1} \tilde{H}_c L_*^2(r_h) j^2 \text{ erg}. \quad (9)$$

In the Blandford-Payne (BP) model extracting the gravitational energy of an accretion disk, the jet power associated with it is calculated as:

$$P_{\text{jet}}^{\text{BP}} \sim \frac{B_z B_\phi^s}{2\pi} R_j \Omega \pi R_j^2, \quad (10)$$

where  $B_\phi = \xi_\phi B_z$  refers to the azimuthal component of the field at the corona surface,  $R_j$  symbolizes the radius of the jet formation region within the corona, and  $\Omega$  signifies the angular velocity of the gas in the corona. Then we can obtain the BP jet power as:

$$P_{\text{jet}}^{\text{BP}} \simeq 3.13 \times 10^{37} \xi_\phi \tilde{\Omega} r_j^{-1/2} m \beta \tau_c \tilde{H}_c \text{ erg s}^{-1}. \quad (11)$$

Given that a substantial part of gravity can be released in the inner region of the accretion disk, specifically, within a radius of about  $2R_{\text{ms}}$ , then  $R_j = 2R_{\text{ms}}$  is considered for calculating the BP jet power.

In the Hybrid model, which is contributed by both BZ mechanism and BP mechanism, we can derive its total jet power for a thin accretion disc:

$$P_{\text{jet}}^{\text{Hybrid}} = 2 \times 10^{47} \text{ erg s}^{-1} \alpha f^2 \frac{B_z}{10^5 \text{ Gauss}} m_9^2 j^2, \quad (12)$$

where  $m_9 = m/10^9$ ,  $\alpha$  serves to establish the effectiveness of the BP jet as a function of spin, and  $f$  refers to the enhancement of the black hole by the disk through the magnetic field.

### 3. Result and Discussion

#### 3.1 Parameters

We derive  $M_7$  ( $= 10^7 M_{\text{sun}}$ ),  $\delta$ ,  $d/R_\gamma$  and  $\Phi$  for every single sources in our sample using Equations (3), and the results are presented in the last four columns in Figure 1. The upper left panel shows the distributions of  $M_7$  for BL Lacs and FSRQs. The ranges are from 0.54 to 99.90 with an average value of  $16.56 \pm 12.74$  and a median of 13.34 for 468 BL Lacs, and from 1.11 to 91.46 with an average value of  $16.38 \pm 9.77$  and a median of 16.24 for 341 FSRQs. A Kolmogorov-Smirnov test (hereafter K-S test) is performed on two sub-samples and suggest that the central black hole mass perhaps plays a less important role in the evolutionary sequence of blazars.

The distributions of  $\delta$  for BL Lacs and FSRQs are displayed in the upper right panel, spanning from 0.15 to 3.84 with an average value of  $1.32 \pm 0.67$  and a median of 1.20 for BL Lacs, and from 0.31 to 7.96 with an average value of  $2.24 \pm 1.10$  and a median of 2.03 for FSRQs. The Doppler factors for FSRQs are on average higher than that for BL Lacs. On the other hand, severally, medians of 1.15, 1.22 and 1.26 for 202 HBLs, 231 IBLs and 35 LBLs are also acquired, revealing that Doppler effect varies in different sub-classes of blazars.

The lower left panel in Figure 1 presents the distributions of  $d/R_g$  for our sample, which are in the scope from 5.12 to 545.66 with a median of 106.48 for BL Lacs, and from 10.21 to 655.97 with

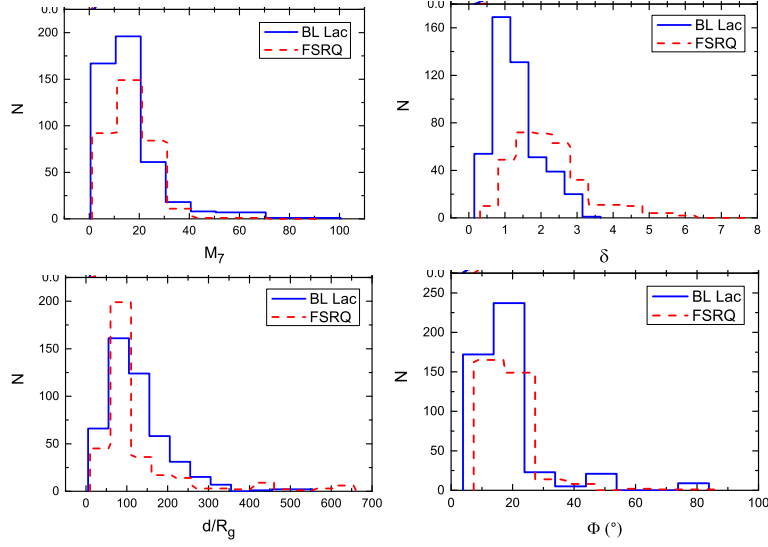


**Figure 1:** Distributions of the upper limit of central black hole mass ( $M_7$ ), Doppler factor ( $\delta$ ), the distance along the axis to the site of the  $\gamma$ -ray production ( $d/R_g$ ), and the propagation angle with respect to the axis of the accretion disk ( $\Phi$ ) for BL Lacs and FSRQs. In this Figure, the *red solid line* stands for BL Lacs and *blue dashed line* for FSRQs.

a median of 80.02 for FSRQs. Finally, the distributions of  $\Phi$  for BL Lacs and FSRQs are exhibited in the lower right panel. The values are in the extent between  $3.84^\circ$  and  $83.97^\circ$  with a median of  $16.33^\circ$  for BL Lacs, and from  $7.33^\circ$  to  $84.31^\circ$  with a median of  $18.08^\circ$  for FSRQs.

### 3.2 Emission Core-Dominance in High Energy Band

The distribution of the  $\gamma$ -ray core-dominance parameter,  $\log R_\gamma$ , for BL Lacs, FSRQs and BCUs is shown in the left panel in Figure 2. We found that the average values of  $\log R_\gamma$  for BL Lacs, FSRQs and BCUs are  $\langle \log R_\gamma \rangle_{\text{BL Lac}} = 2.38 \pm 1.91$ ;  $\langle \log R_\gamma \rangle_{\text{FSRQ}} = 3.07 \pm 2.01$  and  $\langle \log R_\gamma \rangle_{\text{BCU}} = 1.80 \pm 2.42$ , respectively. From the distributions and the K-S test result, we found that  $\langle \log R_\gamma \rangle_{\text{FSRQ}} > \langle \log R_\gamma \rangle_{\text{BL Lac}}$ , indicating that the  $\gamma$ -ray emission of *Fermi*-detected FSRQs are more core dominated than are *Fermi* BL Lacs.

The distribution of the X-ray core-dominance parameter,  $\log R_x$ , for BL Lacs and FSRQs as shown shown in the middle panel in Figure 1. The X-ray core-dominance parameter  $\log R_x$  is in a range of -2.32 to 6.37 with an averaged value of  $\langle \log R_x \rangle = 0.95 \pm 1.48$  for the whole sample. For the two subclasses, we have  $\log R_x = -2.18$  to 6.37 with  $\langle \log R_x \rangle = 1.31 \pm 1.56$  for BL Lacs, and  $\log R_x = -2.31$  to 4.93 with  $\langle \log R_x \rangle = 0.64 \pm 1.35$  for FSRQs. It is found that  $\langle \log R_x \rangle$  in BL Lacs is 2 times greater than  $\langle \log R_x \rangle$  in FSRQs, indicating that the X-ray emissions of *Fermi*-detected BL Lacs are more core dominated than that of *Fermi*-detected FSRQs. We propose that higher  $R$  in BL Lacs than in FSRQs does not imply that the Doppler factor  $\delta$  in BL Lacs is greater than that in FSRQs. It can be explained by the difference of the ratio of intrinsic emissions to the unbeamed emissions ( $f = \frac{L_{\text{r,b}}^{\text{in}}}{L_{\text{r,unb}}}$ ).

The right panel in Figure 1 shows the TeV core-dominance parameter ( $\log R_{\text{TeV}}$ ) for BL Lacs and FSRQs, and their average values are:  $\langle \log R_{\text{TeV}}^{\text{BL}} \rangle = 3.12 \pm 2.83$  and  $\langle \log R_{\text{TeV}}^{\text{FSRQ}} \rangle = 4.80 \pm 1.76$ ,

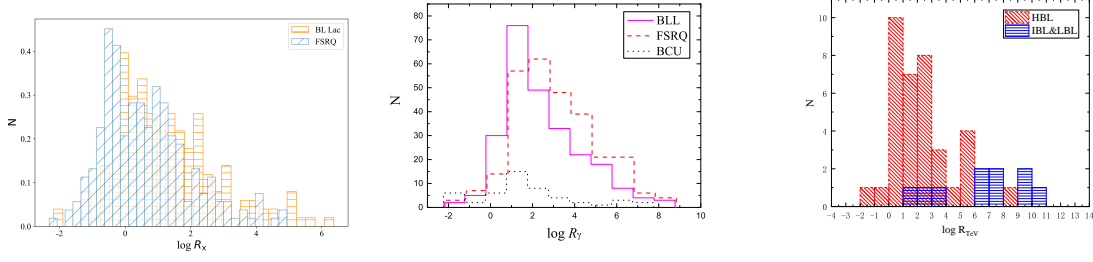


**Figure 2:** Distributions of  $R_\gamma$  for BL Lacs, FSRQs and BCUs in our sample.

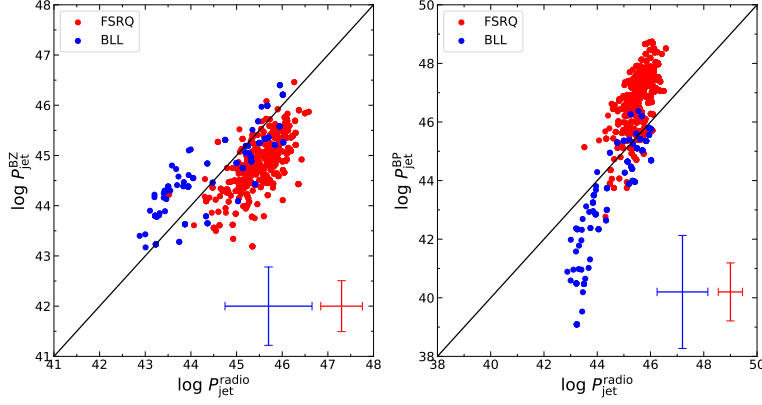


**Figure 3:** The correlation between jet power calculated by radio flux density and that by BP and BZ mechanism. This Figure is adopted from Xie et al. (2024)[14].

which indicates that the mean value of FSRQs is larger than that of BL Lacs. However, there are only 5 FSRQs in our TeV blazar sample.

### 3.3 Jet Mechanism

We calculated and compared the  $P_{\text{jet}}^{\text{radio}}$  with the calculated theoretical BZ and BP jet power. The results of comparison between the observed radio-based jet power ( $P_{\text{jet}}^{\text{radio}}$ ) and the calculated theoretical maximal jet power ( $P_{\text{jet}}^{\text{BZ}}$  and  $P_{\text{jet}}^{\text{BP}}$ ) are shown in Figure 3. In the left panel, 273 of 287 FSRQs lie below the equality line, while 14 lie above the line; 37 of 60 BL Lacs lie above the line, and 23 lie below the line. In the right panel, 264 of 287 FSRQs lie above the equality line, 23 lie below the line; 51 of 60 BL Lacs lie below the line and 9 BL Lacs lie above the line. The results suggest that FSRQ jets are produced by the BP mechanism, while the BZ mechanism might not be sufficient. For BL Lacs, the BZ mechanism may be sufficient for most of BL Lacs to launch jets [14].

## 4. Summary

- We present an effective method by means of the beaming effect to estimate four crucial parameters, including the central black hole mass  $M$ , the Doppler factor  $\delta$ , the location of

$\gamma$ -ray-emitting region  $R_\gamma$ , and the propagation angle with respect to the axis of the accretion disk  $\phi$ , for more than 800 gamma-ray blazars. We put forward an updated demarcation between BL Lacs and FSRQs based on the relation between broad-line region luminosity and disk luminosity both measured in Eddington units, i.e.,  $L_{\text{disk}}/L_{\text{Edd}} = 4.68 \times 10^{-3}$ , indicating that there are some differences between BL Lacs and FSRQs on the accretion power in the disk.

- By adopting a two-component model of emission within jets, we successfully separated the emission of radio, X-ray, GeV and TeV into beamed and unbeamed contributions for the largest sample of Fermi blazars up to now. Our results suggest that the emission is mainly from the core/beamed component in gamma-ray blazars.
- Our results suggest that BL Lac jets are powered by extracting black hole rotation energy, while FSRQ jets are mostly powered by accretion disks. Most of FSRQs can be explained by the BP mechanism, while most of BL Lacs can be explained by the BZ mechanism.

## References

- [1] Urry, C. M., & Padovani, P. 1995, *PASP*, 107, 803
- [2] Fan, J.-H., Bastieri, D., Yang, J.-H., et al. 2014, *RAA*, 14, 1135
- [3] Ghisellini, G., Tavecchio, F., Foschini, L., & Ghirland a, G. 2011, *MNRAS*, 414, 2674, doi: 10.1111/j.1365-2966.2011.18578.x
- [4] Pei, Z., Fan, J., Bastieri, D., Yang, J., & Xiao, H. 2020, *Science China Physics, Mechanics, and Astronomy*, 63, 259511, doi: 10.1007/s11433-019-1454-6
- [5] Abdollahi, S., Acero, F., Ackermann, M., et al. 2020, *ApJS*, 247, 33
- [6] Blandford, R. D., & Znajek, R. L. 1977, *MNRAS*, 179, 433
- [7] Blandford, R. D., & Payne, D. G. 1982, *MNRAS*, 199, 883
- [8] Xiao, H., Ouyang, Z., Zhang, L., et al. 2022, *ApJ*, 925, 40
- [9] Pei, Z. Y. et al. 2022, *ApJ*, 925, 97
- [10] Orr, M. J. L., & Browne, I. W. A. 1982, *MNRAS*, 200, 1067, doi: 10.1093/mnras/200.4.1067
- [11] Pei Z., Fan J., Yang J., Bastieri D., 2020, *PASP*, 132, 114102
- [12] Zeng X., Zhang Z., Pei Z., Xiao H., Fan J., 2022, *ApSS*, 367, 36
- [13] Zhang Z., Zeng X., Pei Z., Xiao H., Ye X., Fan J., 2022, *PASP*, 134, 064101
- [14] Shangchun Xie, Zhihao Ouyang, Jingyu Wu, Hubing Xiao, Shaohua Zhang, Yongyun Chen, Zhijian Luo, and Junhui Fan, 2024, *ApJ*, 976, 78